

Simulation of a Polymer Drop in a Shear Field with Dissipative Particle Dynamics Method

S. Chen^{*}, N. Phan-Thien^{**}, X. J. Fan^{***} and B. C. Khoo^{*}

^{*}Singapore-MIT Alliance, National University of Singapore, Singapore 117576,
smachens@nus.edu.sg; mpekbc@nus.edu.sg

^{**}Division of BioEngineering, National University of Singapore, Singapore 117576, biehead@nus.edu.sg

^{***}Institute of High Performance Computing, 1 Science Park Road, #01-01, The Capricorn,
Singapore Science Park II, Singapore 117528, fanxj@ihpc.a-star.edu.sg

ABSTRACT

The dynamics of polymer drops in micro channel in steady-state and transient shear flow conditions are investigated using the Dissipative Particle Dynamics (DPD) method. The polymer drop is made up of 10% DPD solvent particles and 90% finite extensible non-linear elastic (FENE) bead spring chains. With FENE chains, shear thinning and normal stress difference effects are observed. For a polymer drop in steady-state shear field, the relationship between the deformation rate (D) and the Capillary number (Ca) could be divided into linear and nonlinear regimes. As the shear rate increases further, the drop begins to elongate; a sufficiently deformed drop will break up, and in the mean time, possible coalescence may occur for two neighboring drops. In a shear reversal, an elongated and oriented polymer drop retracts towards a roughly spherical shape. Due to the soft interaction of DPD particles, the tumbling phenomena of the polymer drop is not apparent even for large Ca .

Keywords: Droplets, Suspension, Dissipative Particle Dynamics.

1 INTRODUCTION

Dissipative Particle Dynamics (DPD) [1] has emerged as a promising new technique for modeling rheologically complex liquids, such as liquids with interfaces. However, several DPD simulations considered only a Newtonian drop immersed in an immiscible Newtonian fluid [2-3]. There is still no information about the polymer drops evolution in shear fields with DPD method. In the present study, the DPD method is used to investigate the dynamic behavior of a polymer drop in micro channel under shear field conditions.

2 NUMERICAL SIMULATION

2.1 DPD System

In the DPD system, the basic structural unit is a set of discrete momentum carriers called particles that move in

continuous space and discrete time-steps. The momentum carrier is a coarse grained entity of equal mass m placed in a 3D simulation domain. The particle's motion is assumed to represent the collective dynamic behavior of a very large number of molecules. Three interparticle forces act upon the particles, which are called dissipative force, random force and conservative force. Each particle moves along its new velocity for a certain time-step after the collision of two particles. The computation is carried out by solving Newton's equations of motion for each particle for a large number of time steps, making sure it is sufficient to get convergence of the system properties. The system properties, such as viscosity, pressure and interfacial tensions, could be obtained by statistical average of the positions, velocities or forces of each particle at each time step. DPD conserves not only the number of particles but also the total momentum of the system, and satisfies Galilean invariance, and the detailed balance equations.

2.2 FENE Chain Model

By introducing bead-and-spring type particles, polymers can be simulated with the DPD method. The FENE (finitely extensible nonlinear elastic) model is designed to produce a non-Newtonian fluid that is tractable for computer simulation. The FENE spring force is used to impose a finite maximum extension for the chain segment. In the FENE chain, the force on bead i due to bead j is

$$F_{ij}^s = -\frac{Hr_{ij}}{1-(r_{ij}/r_m)^2} \quad (1)$$

where H is the spring constant, and r_m is the maximum length of one chain segment. The spring force increases drastically with r_{ij}/r_m and becomes infinity as $r_{ij}/r_m = 1$.

2.3 Binary Immiscible Fluids

Immiscible fluid mixtures exist because individual molecules attract similar and repel dissimilar molecules. The miscibility of the two fluids is controlled mainly by the interaction parameter α between the drop and the

surrounding fluids, α is a maximum repulsion between two particles. In order to model immiscible fluids, we adopt the method which introduced a new variable, called the “color” according to Rothman-Keller [4]. When two particles of different color interact, we increase the conservative force, thereby increasing the repulsion, that is,

$$\alpha_{ij} = \begin{cases} \alpha_0 & \text{if particles } i \text{ and } j \text{ are the same color} \\ \alpha_1 & \text{if particles } i \text{ and } j \text{ are different colors} \end{cases} \quad (2)$$

The two phases would be completely miscible if $\alpha_1 \approx \alpha_0$ and almost entirely immiscible if α_1 exceeds α_0 appreciably.

2.4 Simulation Procedure

The channel sizes are $40 \times 20 \times 30$ units (r_c^3), as shown in Fig. 1. In the present study, the polymer drop consists of 118 FENE chains, and each chain is made up of 16 beads. The polymer drop is a solution of 90% concentration. Beside the FENE chains, there are 208 particles representing the solvent within each drop. In essence there are 2096 particles comprising each drop. Fluid occupies the remaining space in the channel, represented by 96000 simple DPD particles. A shear flow is generated by sliding the plates in opposite directions. Periodic boundary conditions are applied on the fluid boundary of the computational domain in the X and Y directions. The solid wall is represented using frozen particles.

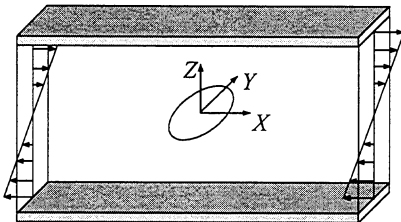


Figure 1: Polymer drop undergoing shear flow between two parallel planes

3 RESULTS AND DISCUSSION

3.1 Rheological Properties

Fig. 2 shows the polymer solution viscosity as functions of the shear rate. It can be clearly seen from this figure that the fluid is shear-thinning for this range of shear rates. The shear-thinning behavior can be described by a power-law relationship as following

$$\eta = A\dot{\gamma}^{-n} \quad (3)$$

with the power-law index n 0.139.

Fig. 3 shows the first (N_1) and second (N_2) normal stress differences against the shear rate. N_1 predicted in the present study is positive, whereas N_2 is almost zero and slightly negative. N_1 can be fitted to a power-law similar to that observed for viscosity in the form $N_1 = B\dot{\gamma}^m$. The value for m is about 1.56 in the present study.

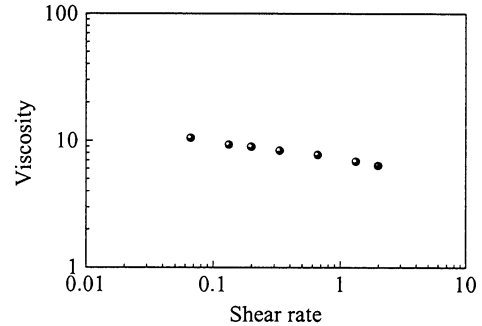


Figure2: Polymer solution viscosity as functions of shear rate

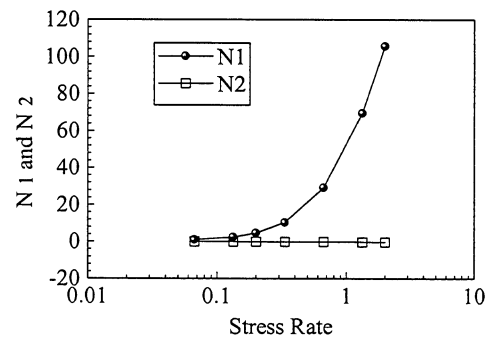


Figure 3: First and second normal stress differences

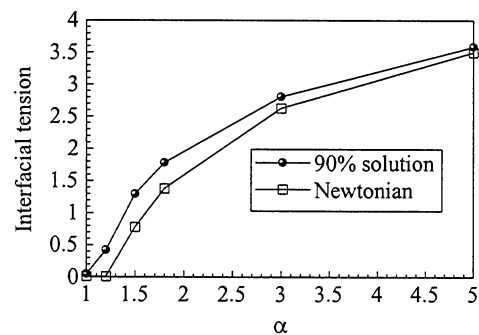


Figure 4: Two immiscible fluids and their interfacial tensions

3.2 Interfacial Tension

The interfacial tension increases with the increasing of α between the two fluids, shown as in Fig. 4. For the same

value of α , the interfacial tension of the fluid with polymer chains is always larger than that of the solvent.

3.3 Drop in a Steady State Shear Field

The first theoretical analysis of drop shape in shear flow was proposed by Taylor, who presented a small deformation analysis restricted to Newtonian fluids. The shape of the sheared drop would be governed by Capillary number,

$$Ca = \frac{\eta_s \dot{\gamma} R}{\Gamma_{AB}} \quad (4)$$

where η_s is the viscosity of the medium, $\dot{\gamma}$ is the shear rate, R is the radius of the undeformed drop, and Γ_{AB} is the interfacial tension. Another dimensionless group governing the shape is the viscosity ratio, $\lambda = \eta_d / \eta_s$, η_d being the viscosity of the drop.

Within the limit of small deformations according to Taylor's theory, the drop is an ellipsoid with the major radius a oriented at an angle θ of 45° with respect to the velocity gradient direction. The degree of deformation is represented by the parameter $D = (a - b)/(a + b)$, where b is the smallest radius of the ellipsoid. Taylor's theory yielded the following well-known expression for the steady-state value of the deformation parameter D as a function of λ and Ca

$$D = \frac{19\lambda + 16}{16\lambda + 16} Ca \quad (5)$$

The predictions of the theory start soon to deviate from experimental observations. This discrepancy is not unexpected, since Taylor's theory is supposed to be valid only in the limit of $Ca \ll 1$.

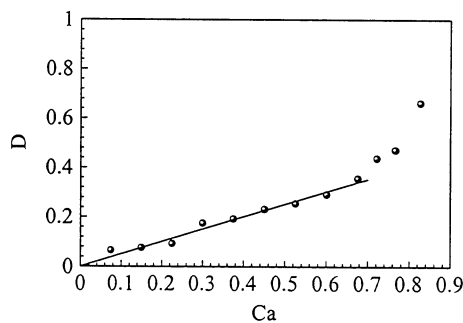


Figure 5: Variation of D with the Capillary number Ca

3.4 Deformation of Drop

In Fig. 5, D is plotted as a function of Ca . The Capillary number is calculated with $\Gamma = 2.806$. Fig. 5 could be

divided into linear and nonlinear regimes according to the relationship between D and Ca , which is in accord with the theoretical prediction. The drop consists of many FENE chains, due to the chain entanglements, the polymer drop is not easy to deform, the Capillary number for the linear regime is $Ca \approx 0.7$, larger than that of the Newtonian drop.

3.5 Drop Breakup

The ellipsoidal shape of the drop distorts with the increasing of shear rate, and necking may develop. When that happens, the drop may break up into several droplets. In the present study, the breakup occurs when $Ca > 0.9$. Fig. 6 shows the breakup process of the drop. The drop is firstly stretched and then breaks up into new droplets. But the droplet 1 is not stable and it coalesces with droplet 2 soon afterward to form a new droplet. In the mean time, a new droplet 3 is developed from the most of the stretched drop. The dynamical equilibrium between breakup and coalescence results in a steady-state average droplet-size distribution, as shown at $t = 780$, two small drops with approximately same size are relatively stable. From Fig. 6 we also noted some threads are developed between the droplets.

Computational results of Clark [3] show that there is a critical Capillary number, Ca^C (the minimum value of Ca required to actuate the breakup process) of about 0.26, for a Newtonian drop. In our simulation the critical Capillary number is 0.9 for the polymeric drop.

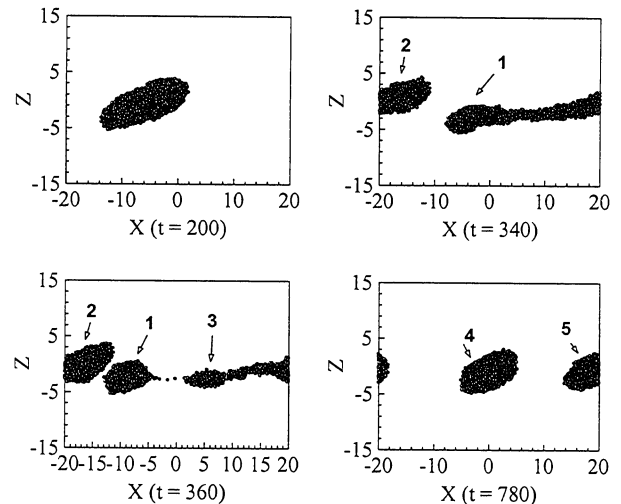


Figure 6: Evolution of a polymer drop breakup under steady state shear field

3.6 Transient Deformation of Polymer Drop under Shear-flow Reversal

In the present study, the shape evolution and orientation of a polymer drop under transient shear-flow

reversal condition are also considered. The shear rate is reversed after a steady state in the deformed drop has been reached. The study of this flow history can provide insight into the basic mechanism of drop dynamics. The sketch for the transient shear flow is shown in Fig. 7. The initial zero shear rate (Region 1) serves to generate an equilibrium state of the drop.

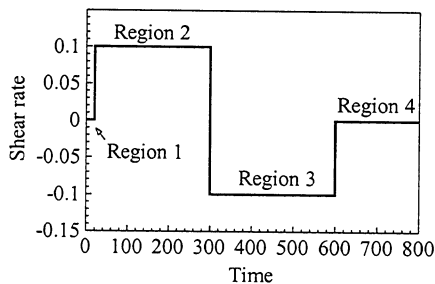


Figure 7: Shear history regimes imposed

Fig. 8 shows the drop deformation as viewed from the vorticity direction (Y direction) under a flow reversal, with shear history as sketched in Fig. 7. During shear rate reversal the elongated oriented drop retracts towards a nearly spherical shape ($t \approx 360$), and then to be stretched again by the flow, changing to a new orientation. In Fig. 8, $Ca \approx 0.45$. The same phenomena have been observed by Guido et al [5] under flow condition where there is a shear rate reversal. In their case, $Ca \approx 0.20$, the drop is Newtonian. Considering the polymer drop in the present study, Ca is expected and indeed it is higher.

In Guido et al's [5] work, another case was reported and it is quite different from the previous one that has just been discussed. The drop remains elongated throughout the evolution for $Ca \approx 0.4$. The drop's major axis rotates counter-clockwise towards the new steady state. The path of this opposite to that one would observe for a rigid elongated body subjected to the same flow field. In the present study, when $Ca \approx 0.6$, However, the tumbling behaviour has not been observed apparently. This may be due to the fact that in DPD system the repulsion force is soft when compared to the real molecule force.

4 CONCLUSIONS

Using the Dissipative Particle Dynamics, we investigate the evolution of polymer drop under a shear field. The appropriate non-Newtonian behaviour, shear thinning and normal stress difference, are all observed by using the FENE chain model into the DPD system. In the present study, both viscosity and first normal stress difference obey the power law relationship with the shear rate, with the exponents being -0.139 and 1.56 respectively. Rothman-Keller "color" scheme is used to model the immiscibility of two fluids by changing a parameter α . The interfacial tension of the polymer drop is always greater than that of

Newtonian drop keeping all other conditions. Because of the entanglement of the chains, the linear regime for a polymeric drop under a steady state shear flow is considerably larger than that of Newton drop. The dynamical equilibrium between breakup and coalescence results in a steady-state average droplet-size distribution. The threads occurring in the breakup process could be simulated in the DPD system. For the polymer drop under shear flow reversal, the deformed polymer drop retracts towards a roughly spherical shape firstly, and then it deforms and orients in a new direction. The tumbling phenomena of the polymer drop is not apparent even Ca is large enough; this may be due to the soft repulsion forces between the momentum carriers.

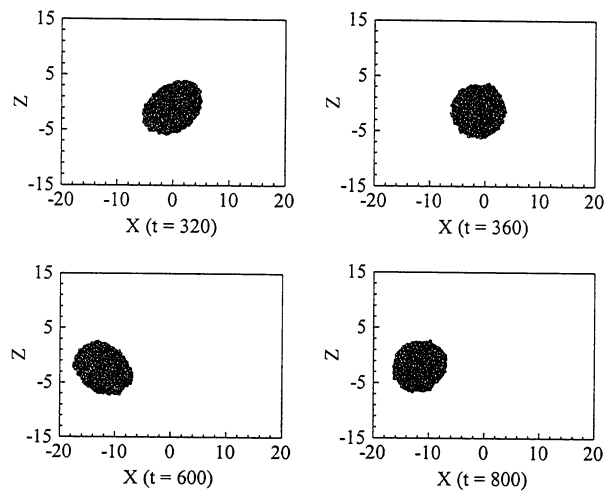


Figure 8: Evolution of a polymer drop under flow reversal

REFERENCES

- [1] P. J. Hoogerbrugge and J. M. V. A. Koelman, "Simulating Microscopic Hydrodynamic Phenomena with Dissipative Particle Dynamics", *Europhys. Lett.*, 19, 155, 1992.
- [2] J. L. Jones, M. Lal, J. N. Ruddock and N. A. Spenley, "Dynamics of a drop at a liquid/solid interface in simple shear fields: a mesoscopic simulation study". *Faraday Discuss.*, 112, 129, 1999.
- [3] A. T. Clark, M. Lal, J. N. Ruddock, and P. B. Warren, "Mesoscopic simulation of drops in gravitational and shear Fields", *Langmuir*, 16, 6342, 2000.
- [4] K. E. Novik and P. V. Coveney, "spinodal decomposition of off-critical quenches with a viscous phase using dissipative particle dynamics in two and three spatial dimensions", *Physical review E*, 61, 435, 2000.
- [5] S Guido, M. Minale and P. L. Maffettone, "Drop shape dynamics under shear-flow reversal", *J. Rheol.*, 44, 1385, 2000.